International Journal of Hybrid Information Technology
Vol.8, No.3 (2015), pp.307-320
http://dx.doi.org/10.14257/ijhit.2015.8.3.27

Mixing Matrix Estimation based on Directional Density Detection and Hough Transform

SUN Jie-Di[1], LI Yu-Xia[1], WEN Jiang-Tao[2] and YAN Sheng-Nan[1]

(1.School of Information Science and Engineering, Yanshan University, Qinhuangdao 066004, China
sjdwjt@ysu.edu.cn
2. Key Laboratory of Measurement Technology and Instrumentation of HeBei Province, Yanshan University, Qinhuangdao, 066004, China)

Abstract

Mixing matrix estimation (MME) algorithm was proposed for the mixing matrix estimation problem of underdetermined blind source separation. The algorithm is based on a combination of processing of isolated time–frequency points from local directional density detection and Hough transform (HT). Firstly, signal sparsity was strengthened through the processing of single-source time–frequency points in the transform domain. Next, HT was applied to the directional straight lines in the scatter plot and realized the spatial transformation. The number of source signals and mixing matrix were estimated by determining the local maxima of cumulative array. To deal with the peak values clustering issue that commonly arises with HT, the local directional density detection method was used to identify and eliminate isolated time–frequency points. HT was then used to improve the accuracy of MME. The experimental results indicate that the proposed method is able to achieve MME under the condition when the number of source signals is unknown. Further, the accuracy of estimation is better than other commonly-used methods such as K-means.

Keywords: *underdetermined blind source separation, mixing matrix estimation, Hough transform, directional density detection, isolated time-frequency coefficients*

1. Introduction

Blind source separation is used when the source signals and transmission channel parameters are unknown. During the process, the observed signals alone are used to restore the input source signals, based on the latter's statistical characteristics. It has become a popular research topic in recent years due to its wide applications in various fields, including digital communication, speech recognition, and array signal processing.

A problem faced during underdetermined blind source separation (UBSS) is the number of observed signals being less than that of the source signals. Most of the existing research to solve this problem focuses on the sparse component analysis (SCA) method, which uses the sparsity characteristics of signals. A two-step method is commonly involved: (a) mixing matrix estimation (MME), and (b) source signals restoration. The former is an important step to achieve UBSS. The accuracy of the estimation in turn directly affects the quality of signal separation.

Using signal sparsity, Literature [1] proposed an underdetermined MME algorithm based on potential functions. However, this method does not provide any theoretical guidance for the selection of the potential function parameters. Literature [2] combines K-means clustering with Hough transform (HT) to estimate the mixing matrix. Since the K-means algorithm relies on both the selection of the initial cluster center and prior knowledge of the number of source signals, it cannot be applied when the number of

ISSN: 1738-9968 IJHIT

source signals is unknown. Literature [3, 4] proposed the probabilistic statistics method to estimate the number of source signals, but its application cannot be extended to high-dimension domains. It also imposes greater requirements on signal sparsity [5-8]. Some scholars had recommended the use of the single-source time–frequency point method [9-11] to make the signal sparsity requirement less stringent and strengthen signal sparsity. The issues with this method include the multiplicity of definition and difficulty in meeting the eligible conditions.

In this study, a MME algorithm based on isolated time–frequency points detection and HT was proposed. It addresses several inadequacies of traditional clustering methods, including weak signal sparsity, dependence on the selection of the initial cluster center, and requirement to determine the number of source signals in advance. First, a method to process the single-source time–frequency points in the transform domain was used to strengthen signal sparsity. Next, HT converted the directional detection of straight lines to the detection of local maxima in the transform domain, thereby achieving the aim of MME. The further elimination of isolated time–frequency points was proposed to address peak values clustering in the HT results.

2. Signal Sparsity Strengthen based on Single-source Time–frequency Points Processing

When the impact of noise is not considered, the formula for the UBSS instantaneous mixing model is as follows:

$$\boldsymbol{x}(t) = \boldsymbol{A}\boldsymbol{s}(t), \quad t=1,2, \cdots ,T \tag{1}$$

where $\boldsymbol{x}(t)=[x_1(t),x_2(t), \cdots ,x_m(t)]^{\mathrm{T}}$, m is the number of observed signals; $\boldsymbol{A}=[a_1,a_2,\cdots,a_n]$ is the mixing matrix, $\boldsymbol{A}\in R^{m\times n}$. For $\boldsymbol{s}(t)=[s_1(t),s_2(t),\cdots,s_n(t),]^{\mathrm{T}}$, n is the number of unknown source signals; $m<n$ represents a UBSS problem. A sparse signal refers to sample point value approaches or reaches zero at the majority of the sampled points and with values that are not zero for only a few sampled points. In other words, when the source signal becomes sparse, there is usually only one source signal with a larger value at time t_K , namely

$$\frac{x_1(t_K)}{a_{1i}} = \frac{x_2(t_K)}{a_{2i}} = \cdots = \frac{x_m(t_K)}{a_{mi}} \tag{2}$$

It can be seen from Formula (2) that the observed signals are distributed along a straight line that passes through the origin. The direction of the straight line is determined by column vector $\boldsymbol{a}_i$ of the mixing matrix. Hence, sparse signals are characterized by linear clustering, while the degree of linear clustering directly affects the estimation accuracy of the mixing matrix.

Most signals in the transform domain have the characteristic of sparsity. This study focuses on the processing of sparsity in the transform domain. By applying short-time Fourier transform (STFT) to Formula (1), it can obtain:

$$\boldsymbol{X}(t,k) = \sum_{i=1}^{n} \boldsymbol{a}_i S_i(t,k) \tag{3}$$

where $\boldsymbol{X}(t,k)$ represents the STFT coefficient of the observed signals and $S_i(t,k)$ represents the STFT coefficient of the i^{th} source signal.

After signals with weak sparsity are transformed to the time–frequency domain, the direction of the observed signals still remains unclear. This indicates the presence of some interference time-frequency points. For any time-frequency points in time-frequency domain, when only one source signal exists as the valid time-frequency point, it is defined

as a single-source point. In this study, the detection of such single-source points is used to strengthen signal sparsity.

Assuming that in the time–frequency domain, only one signal s_1 exists at the time–frequency point (t_1, k_1), then Formula (3) can be expressed as:

$$\boldsymbol{X}(t_1, k_1) = \boldsymbol{a}_1 S_1(t, k) \tag{4}$$

$R\{\cdot\}$ and $I\{\cdot\}$ are used to represent the real and imaginary parts of Formula (4), respectively. From the linear clustering characteristic of sparse signals, the component weight ratio of both $R\{\boldsymbol{X}(t_1, k_1)\}$ and $I\{\boldsymbol{X}(t_1, k_1)\}$ is $\boldsymbol{a}_1$. If there are multiple source signals s_1 and s_2 at the time–frequency point (t_2, k_2), then the respective observed vectors of the real and imaginary portions are:

$$R\{\boldsymbol{X}(t_2, k_2)\} = \boldsymbol{a}_1 R\{S_1(t_2, k_2)\} + \boldsymbol{a}_2 R\{S_2(t_2, k_2)\} \tag{5}$$

$$I\{\boldsymbol{X}(t_2, k_2)\} = \boldsymbol{a}_1 I\{S_1(t_2, k_2)\} + \boldsymbol{a}_2 I\{S_2(t_2, k_2)\} \tag{6}$$

If the component weight ratios of the real and imaginary portions of the observed vector are similar, then:

$$\frac{R\{S_1(t_2, k_2)\}}{I\{S_1(t_2, k_2)\}} = \frac{R\{S_2(t_2, k_2)\}}{I\{S_2(t_2, k_2)\}} \tag{7}$$

This means that $R\{X_i\}/I\{X_i\} = R\{X_j\}/I\{X_j\}$ must be satisfied, where $i, j \in [1, m]$且$i \neq j$. The probability that Formula (7) can be established is extremely low. Considering the actual error and setting the range of threshold value ε as 0.01–0.1 [11], the following is obtained:

$$\left| \frac{R\{X_i\} / I\{X_i\} - R\{X_j\} / I\{X_j\}}{R\{X_i\} / I\{X_i\} + R\{X_j\} / I\{X_j\}} \right| < \varepsilon \tag{8}$$

Formula (8) is for the detection of single-source points. To improve the impact of low-energy time-frequency points, these are processed by Formula (9):

$$\left\| \boldsymbol{X}(t, k) \right\| > \lambda \cdot \max \left\| X(t, k) \right\| \tag{9}$$

In the formula, $\lambda \in (0,1)$. After these treatments, signal sparsity would increase significantly. This provides the foundation for the estimation of the mixing matrix.

3. Mixing Matrix Estimation based on Isolated Points Detection and HT

3.1 Directional Straight Line Transformation based on HT

When estimating a mixing matrix, traditional K-means clustering algorithm has the deficiencies, specifically it needs to select the initial cluster center and has prior knowledge of the number of source signals. Combined with the spatial transformation characteristics of HT, an MME algorithm based on the number of sources and HT was proposed.

HT is a mapping method that transforms data in the graphical domain to the parameter domain by making the objects in the former undergoes a particular form of coordinate transformation. Subsequently, all the points on the specified curves in the original graphical domain are clustered at particular locations in the transform domain, forming a series of local cumulative maxima.

It assumes that a particular straight line passing through the point (x_1, x_2) in the original graphical domain is $x_2 = ax_1 + b$. Through coordinate transformation, it is

mapped onto the transform domain ρ-θ, and transformed into the corresponding polar coordinates:

$$\rho = x_1 \sin\theta + x_2 \cos\theta \tag{10}$$

Formula (10) is the HT of the point (x_1, x_2), where θ is the angle between the straight line and the x_1 axis, and $\tan(\theta) = x_2 / x_1$.

Considering the application of HT to MME, coordinate transform is used to convert those original domain points with collinear lines to intersecting curves in the parameter domain. Since sparse signals have the characteristic of linear clustering, the intersections of the curves are added up to cumulatively form local maxima. The number of source signals can then be determined by counting the number of local maxima. The column vector of the mixing matrix can be realized by detecting the maxima locations.

Since sparse signals have the characteristic of linear clustering, the observed data in UBSS are mainly concentrated along *n* number of straight lines. Hence, the linear vector $\boldsymbol{l}$ can be expressed as:

$$\boldsymbol{l} = \begin{bmatrix} \sin\theta_1 \sin\theta_2 \sin\theta_3 \cdots \sin\theta_{m-1} \\ \cos\theta_1 \sin\theta_2 \sin\theta_3 \cdots \sin\theta_{m-1} \\ \cos\theta_2 \sin\theta_3 \cdots \sin\theta_{m-1} \\ \vdots \\ \cos\theta_{m-2} \sin\theta_{m-1} \\ \cos\theta_{m-1} \end{bmatrix} \tag{11}$$

where $\|\boldsymbol{l}\| = 1$ and $(\theta_1, \theta_2, \cdots \theta_{m-1}) \in [0, \pi)^{m-1}$. After the straight lines are converted to transform domain ρ-θ, ρ can be expressed as:

$$\rho = \boldsymbol{l}^{\mathrm{T}} \boldsymbol{x} \tag{12}$$

The problem of peak values clustering often occur during the HT algorithm calculates the local maxima in the transform domain. The single-source time-frequency points are symmetrically applied onto the upper half surface and followed by HT, the scatter plot of single source points and local maximum distribution are shown in Figure 1:

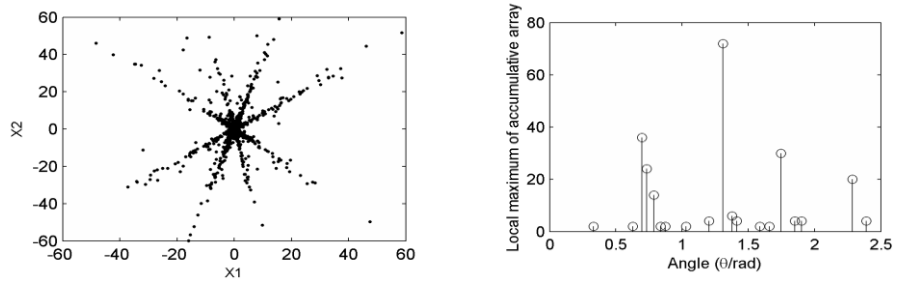

(a) Scatter plot of single source TF points (b) Local maximum distribution

Figure 1. Peak values Cluster of HT Result

Figure 1 illustrates that the existence of isolated points caused the aggregation of the time-frequency points in the normalized scatter plot to be unclear. Therefore, the use of HT to add up the local maxima resulted in the problem of local peak values clustering. This makes accurate estimation of the number of source signals difficult.

3.2. Mixing Matrix Estimation based on Isolated Points Detection

The primary causes of local peak values clustering are the relative lack of time-frequency points and lack of clarity in the linear clustering characteristics, as well as deviations from the main direction of the column vectors of the mixing matrix. These

invalid time-frequency points are defined as isolated time-frequency points. To eliminate the peak values clustering, these isolated points are removed through the local directional time-frequency density detection. Consequently, the accuracy of both the number of source signals and MME are increased.

Single-source point detection in Formula (9) removes the low-energy points, giving N number of time-frequency points aggregated to form $\boldsymbol{X} = \{x_1, x_2, \cdots, x_N\}$. ϕ_{ij} represents the angle between the random time-frequency points x_i and x_j of the observed signals, where $i, j \in N$. The vector direction of time-frequency point x_i is designated as the central direction. The fan-shaped region, which has a central angle of φ, contains the set of time-frequency points $C_i(\varphi) = \{\phi_{ij} \le \varphi, \quad i, j \in N\}$, where φ is a pre-set angle with a small value and should be smaller than the smallest angle in the column vectors of the mixing matrix.

Since the actual observed signal points are concentrated along the corresponding straight lines in the column vectors of the mixing matrix, the directional straight lines of the column vectors will have a certain width. To be precise, the value of φ should be smaller than the width of the straight lines. $N(C_i(\varphi))$ represents the number of time-frequency points within the set $C_i(\varphi)$. The function for local directional time-frequency density is:

$$D_i(\varphi) = \frac{N(C_i(\varphi))}{N} \tag{13}$$

Formula (13) indicates that $D_i(\varphi)$ is positively correlated to the density of the local directional time-frequency points. This shows that x_i reflects the clustering level of time–frequency points in the vector direction. Setting the threshold as δ, when $D_i(\varphi)$ is lower than δ, the time-frequency points in local direction are deemed to be isolated and eliminated. The remaining time-frequency points are valid points and marked as set $\tilde{X}$.

$$\tilde{X} = \{x_i \mid D_i(\varphi) > \delta, i \in N\} \tag{14}$$

After the transformation results of Figure 1 have undergone isolated points detection processing and HT, the results are as shown in Figure 2:

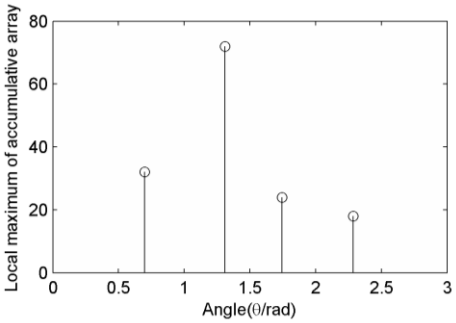

Figure 2. Local Maxima Distribution after Removing Isolated Points

Comparing Figures 1(b) and 2, it can be seen that the proposed processing method effectively prevented peak values clustering and accurately estimated the number of source signals to facilitate following MME.

The steps of proposed method are as follow:

(1): STFT is used to transform the observed signals to the time-frequency domain;

(2): Single-source time-frequency points and low-energy points processing is used to enhance signal sparsity.

(3): Determine the density of local directional time-frequency points and remove isolated points. Then perform HT and determine the maxima of the accumulation arrays within the transform domain.

(4): Determine the number of source signals based on the number of obtained local maxima. Compute the coordinate parameters of the local maxima and the straight line vectors. Finally achieve the estimation of mixing matrix $\boldsymbol{A}$.

4. Results and Analysis

Simulations and analyses were conducted using two experiments (details to be provided later) to verify the validity of the proposed algorithm. Normalized mean square error and deviation angle were used to evaluate the MME performance.

Normalized mean square error is defined as:

$$NMSE = 10\log_{10}\left(\frac{\sum_{i=1}^{m}\sum_{j=1}^{n}\left(\hat{a}_{ij}-a_{ij}\right)^2}{\sum_{i=1}^{m}\sum_{j=1}^{n}a_{ij}^{\ 2}}\right) \tag{15}$$

where m and n denote the number of rows and columns in mixing matrix $\boldsymbol{A}$, respectively; and $\hat{a}_{ij}$ and a_{ij} denote the element in the i^{th} row and j^{th} column of mixing matrix $\hat{\boldsymbol{A}}$ and the original mixing matrix $\boldsymbol{A}$, respectively. The smaller the value of NMSE, the more accurate is the estimation capabilities of $\hat{\boldsymbol{A}}$.

The deviation angle is expressed as follows:

$$ang\left(\boldsymbol{a},\hat{\boldsymbol{a}}\right) = \frac{180}{\pi}\arccos\left(\frac{<\boldsymbol{a},\hat{\boldsymbol{a}}>}{\|\boldsymbol{a}\|\cdot\|\hat{\boldsymbol{a}}\|}\right) \tag{16}$$

where $\boldsymbol{a}$ represents the column vectors in $\boldsymbol{A}$ and $\hat{\boldsymbol{a}}$ represents the corresponding column vectors of $\boldsymbol{a}$ in $\hat{\boldsymbol{A}}$. The smaller the deviation angle, the better is the capability of $\hat{\boldsymbol{A}}$.

4.1. Results and Analysis of Experiment 1

The source signals were three different voice clips, each with a data length of 40,000. Formula (1) was used to mix the clips into two observed signals, namely, $m=2, n=3$. The randomly selected mixing matrix $\boldsymbol{A}$ is:

$$\boldsymbol{A} = \begin{bmatrix} -0.7067 & 0.2594 & 0.9665 \\ 0.7073 & 0.9650 & 0.2595 \end{bmatrix}$$

The observed signals obtained after the mixing are shown in Figure 3:

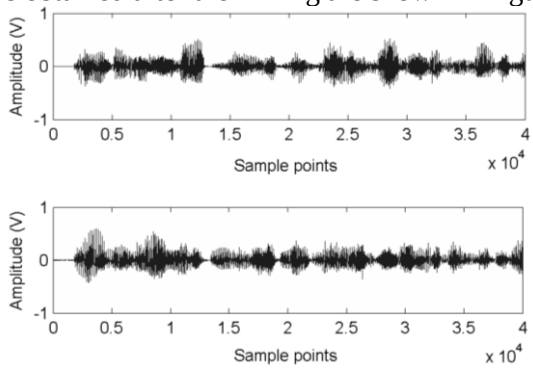

Figure 3. Observed Signals Waveform in Time Domain

Figure 4 shows the scatter plots of observed signals in time domain and the time-frequency domain after STFT transformation:

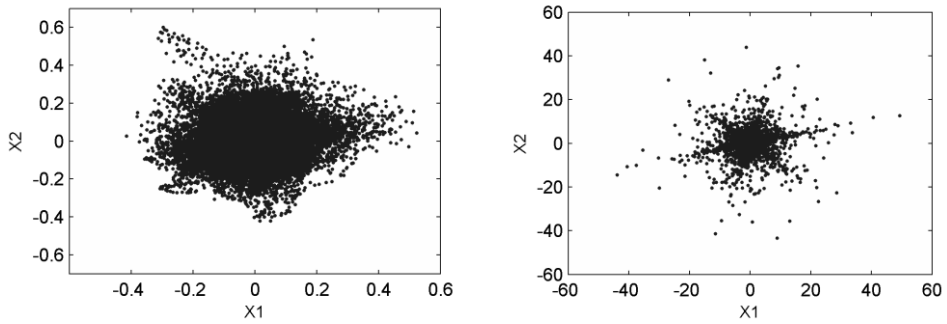

(a)Scatter plot in time domain (b)Scatter plot in time-frequency domain

Figure 4. Scatter Plots of Observed Signals in Time Domain and Time-Frequency Domain

The Figure shows that the direction of the observed signals in the time-frequency domain is weak. Then the single-source time-frequency points processing method was used to enhance signal sparsity. During single-source points processing, it adopted ε=0.06 and the obtained scatter plot of single-source time-frequency points is shown in Figure 5(a). The range of λ is usually 0.05–0.1 [3]. For this study, $\lambda = 0.1$ was adopted. After the dataset was normalized and HT was performed, β was set. Through a large number of experiments and actual conditions $\beta = 180$ was adopted. The local maxima distribution of HT is shown in Figure 5(b):

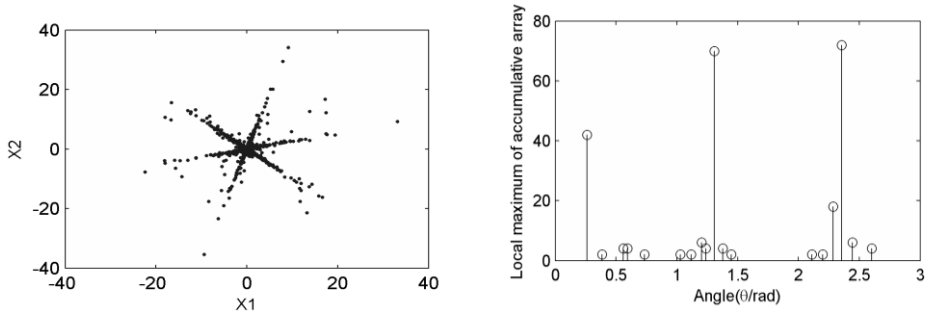

(a) Scatter plot of single source TF points (b) Local maximum distribution

Figure 5. Scatter Plots of Enhanced Observed Signals Sparsity

After the single-source points detection and processing, a small number of time-frequency points still deviated from the direction of the straight lines. This led to peak values clustering in the HT results and affected the estimation of the number of source signals. The proposed local directional time-frequency density detection method was then used to remove the isolated points, with φ=1° . The magnitude of δ determines the number of data points removed. Usually, $\delta \in [\min(D_i(\varphi)), \text{mean}(D_i(\varphi))]$. The ratio between the number of δ counted and the remaining time-frequency points are shown in Figure 6:

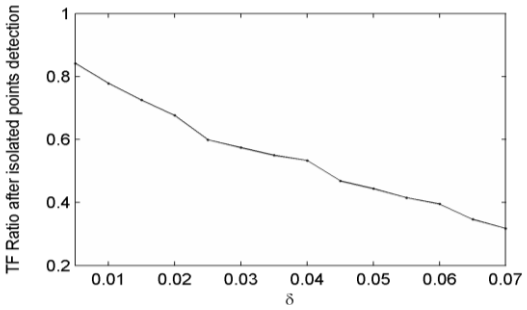

Figure 6. Curve of TF Points Changing with δ

It can be seen from the figure that as δ increases, the percentage of remaining time-frequency points relative to the total number of single-source points decreases. Most of the isolated points are removed when the percentage stabilizes. When δ=0.025 , the percentage tends to decrease in a slow but steady manner. Hence, δ=0.025 was adopted. The normalized scatter plot after removal of the isolated points and the results after HT are shown in Figure 7:

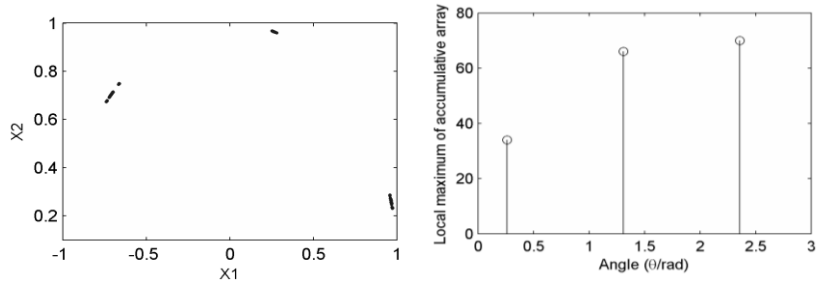

(a) Scatter plot of normalization (b) Local maximum distribution

Figure 7. Local Maximum Distributions after Removing Isolated Points

Figure 7 shows that data clustering becomes clearer after removal of the isolated points. Next, HT was used to resolve the issue of peak values clustering. The determination of local maxima facilitated the accurate estimation of the number of source signals, after which the corresponding coordinate parameters of the local maxima were identified. Substituting that into Formula (11) gives the corresponding column vectors of the straight lines, thereby obtaining the mixing matrix $\hat{A}_1$ of A :

$$\hat{A}_1 = \begin{bmatrix} -0.7071 & 0.2588 & 0.9659 \\ 0.7071 & 0.9659 & 0.2588 \end{bmatrix}$$

To illustrate the validity of the proposed algorithm, the mixing matrices obtained through K-means and K-Hough [3] were compared. After the removal of isolated points, the data underwent K-means clustering. This is named the K-means2 algorithm, which gives the mixing matrix $\hat{A}_2$:

$$\hat{A}_2 = \begin{bmatrix} -0.7071 & 0.2622 & 0.9658 \\ 0.7070 & 0.9650 & 0.2591 \end{bmatrix}$$

The traditional clustering method was unable to eliminate the isolated points. That is named the K-means1 algorithm, which gives the mixing matrix $\hat{A}_3$:

$$\hat{A}_3 = \begin{bmatrix} -0.7025 & 0.2736 & 0.9419 \\ 0.7053 & 0.9580 & 0.3074 \end{bmatrix}$$

$\hat{A}_4$, the mixing matrix obtained through the K-Hough algorithm, is:

$$\hat{\boldsymbol{A}}_4 = \begin{bmatrix} -0.6947 & 0.2588 & 0.9659 \\ 0.7193 & 0.9659 & 0.2588 \end{bmatrix}$$

To accurately compare the estimation accuracy of the various algorithms, the results were substituted into Formulas (15) and (16) to calculate and compare the NMSE and deviation angles between the estimated and original mixing matrices. The results are stated in Table 1:

Table 1. Comparison with Estimated $\hat{A}$ and Original A

Comparison methods	Angle between mixing matrix corresponding column vectors (°)			NMSE (dB)
	$ang\left(\mathbf{a}_1,\hat{\mathbf{a}}_1\right)$	$ang\left(\mathbf{a}_2,\hat{\mathbf{a}}_2\right)$	$ang\left(\mathbf{a}_3,\hat{\mathbf{a}}_3\right)$	
K-Hough	0.9724	0.0466	0.0298	-40.1465
K-means1	0.0977	0.8991	3.0566	-29.7252
K-means2	0.0203	0.1609	0.0007	-55.3761
Proposed method	0.0162	0.0406	0.0188	-63.3725

It is obvious from the table that the removal of isolated points significantly increased the accuracy of the MME and resolved the issue of peak values clustering. This validated the necessity of using isolated points detection and eliminating isolated points. Further, on the basis of accurately estimating the number of source signals, the HT algorithm was able to further enhance the accuracy of the MME. The results of the experiment indicate that the proposed algorithm has a higher degree of accuracy during estimation.

4.2. Results and Analysis of Experiment 2

The source signals for Experiment 2 were the FourVoices voice signals from Literature [1], which have relatively weak sparsity. Four segments of signals, each with a data length of 63,856, were mixed into three-channel observed signals using Formula (1), that is, $m = 3, n = 4$. The randomly selected mixing matrix $\boldsymbol{A}$ is:

$$\boldsymbol{A} = \begin{bmatrix} 0.7110 & 0.2881 & -0.6722 & 0.4539 \\ 0.1770 & 0.9421 & 0.6490 & 0.3952 \\ 0.6818 & 0.1739 & 0.3578 & 0.7991 \end{bmatrix}$$

The observed signals obtained after the mixing are shown in Figure 8:

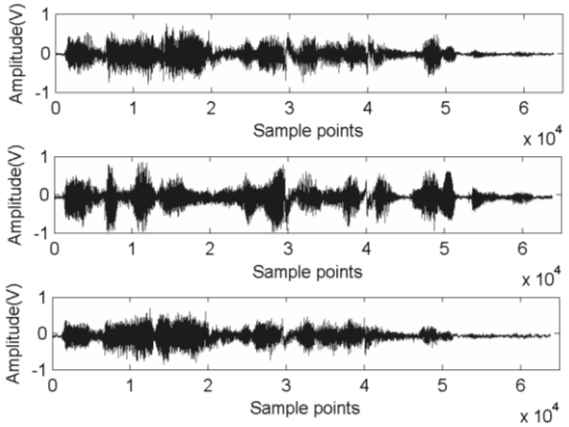

Figure 8. Observed Signals Waveform in Time Domain

After the observed signals have been transformed to the time-frequency domain, the single-source points were detected and normalized before directly undergoing HT. The results are shown in Figure 9:

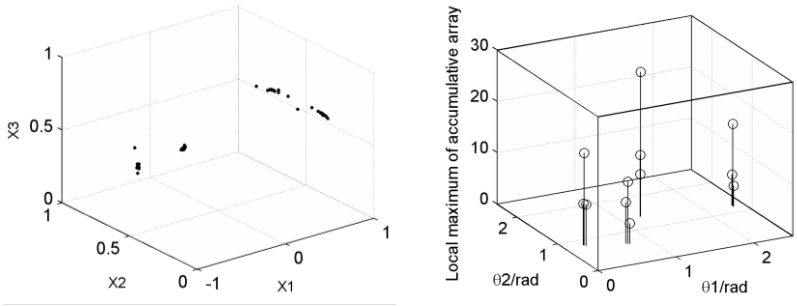

(a) Scatter plot of normalization (b) Local maximum distribution

Figure 9. Local Maximum Distribution of Direct HT without Removal of Isolated Points

Some remnant isolated points from the normalization process in Figure 9 led to the issue of peak values clustering in the HT results. These prevented the accurate estimation of the number of source signals and must be eliminated. The ratio between the number of δ counted and the remaining time-frequency points was set at δ=0.02. The normalized figure after the removal of isolated points and undergoing HT is shown in Figure 10:

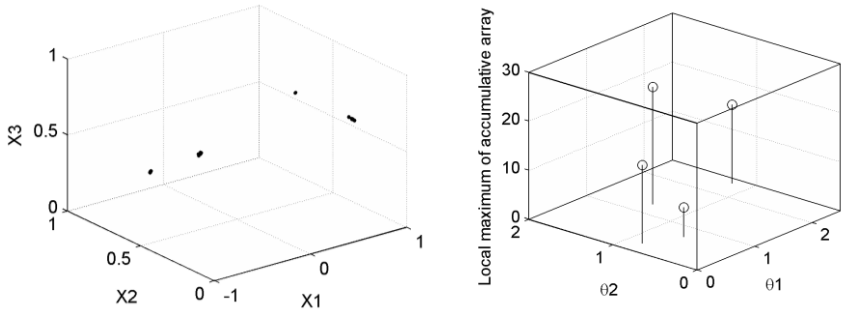

(a) Scatter plot of normalization (b) Local maximum distribution

Figure 10. HT Local Maximum Distribution after Removal of Isolated Points

Comparing Figures 9 and 10, it is seen that the removal of isolated points before undergoing HT can eliminate peak values clustering and lead to an accurate estimation of the number of source signals. The mixing matrix $\hat{\boldsymbol{A}}_1$ obtained through the proposed algorithm is:

$$\hat{\boldsymbol{A}}_1 = \begin{bmatrix} 0.7096 & 0.2879 & -0.6716 & 0.4542 \\ 0.1769 & 0.9418 & 0.6485 & 0.3948 \\ 0.6820 & 0.1736 & 0.3584 & 0.7986 \end{bmatrix}$$

The mixing matrix $\hat{\boldsymbol{A}}_2$ obtained from the K-means 2 algorithm is:

$$\hat{\boldsymbol{A}}_2 = \begin{bmatrix} 0.7092 & 0.2894 & -0.6670 & 0.4515 \\ 0.1781 & 0.9409 & 0.6520 & 0.3961 \\ 0.6820 & 0.1755 & 0.3604 & 0.7996 \end{bmatrix}$$

The mixing matrix $\hat{\boldsymbol{A}}_3$ obtained from the K-means 1 algorithm is:

$$\hat{\boldsymbol{A}}_3 = \begin{bmatrix} 0.7062 & 0.2885 & -0.6562 & 0.4602 \\ 0.1916 & 0.9414 & 0.6623 & 0.4029 \\ 0.6800 & 0.1744 & 0.3511 & 0.7870 \end{bmatrix}$$

The mixing matrix $\hat{\boldsymbol{A}}_4$ obtained from the K-Hough algorithm is:

$$\hat{\boldsymbol{A}}_4 = \begin{bmatrix} 0.7096 & 0.2879 & -0.6601 & 0.4542 \\ 0.1769 & 0.9418 & 0.6601 & 0.3948 \\ 0.6820 & 0.1736 & 0.3584 & 0.7986 \end{bmatrix}$$

Formula (15) was used to calculate the NMSE of the estimation results with different methods. Comparing the results is used to evaluate the capabilities of the various algorithms. Table 2 shows the results:

Table 2. NMSE Comparison with Estimated $\hat{A}$ and Original A (dB)

Comparison methods	K-Hough	K-means1	K-means2	Proposed method
NMSE	-41.6683	-36.1867	-48.2583	-60.3433

The comparative results of the deviation angles in Experiment 2 are shown in Table 3:

Table 3. Deviation Angles Comparison with Estimated $\hat{A}$ Original A (°)

Comparison methods	Angle between mixing matrix corresponding column vectors			
	$ang\left(\mathbf{a}_1,\hat{\mathbf{a}}_1\right)$	$ang\left(\mathbf{a}_2,\hat{\mathbf{a}}_2\right)$	$ang\left(\mathbf{a}_3,\hat{\mathbf{a}}_3\right)$	$ang\left(\mathbf{a}_4,\hat{\mathbf{a}}_4\right)$
K-Hough	0.0639	0.0147	0.9406	0.0325
K-means1	0.8797	0.0476	1.2300	0.8741
K-means2	0.1086	0.1339	0.3732	0.1484
Proposed method	0.0639	0.0147	0.0482	0.0325

Summarizing the aforementioned, it can be concluded that after extending the observed signals into a three-dimensional domain and using the proposed algorithm, the accuracy of the resultant MME was substantially improved. A comparison of the different experimental results proved the validity of the need for isolated points detection, as well as the superiority of the HT algorithm. Overall, the effectiveness of the proposed combination of the local directional time–frequency density detection method and the HT algorithm has been proven.

5. Conclusion

In this study, we used the single-source point detection method to process the transformed results of STFT and enhance signal sparsity. HT was used to convert and process the straight lines in the domain into local accumulated values within the parameter domain, thereby resolving the issue of the unknown number of source signals. The local directional time–frequency density detection method was used to eliminate isolated time–frequency points and the effect of peak values clustering in the HT results. This improved the accuracy when estimating the number of source signals, as well as that of the resultant MME. The experimental results indicate that compared to the commonly-used K-means clustering algorithm and K-Hough algorithm, the proposed algorithm greatly improves the accuracy of the MME.

Acknowledgements

The Project Supported by National Natural Science Foundation of China No. 51204145, Natural Science Foundation of Hebei Province of China No. E2013203300 and Science and Technology Research and Development Program of Qinhuangdao No.201302A033.

Reference

[1] P. Bofill and M. Zibulevsky, "Underdetermined blind source separation using sparse representations", Signal Processing, vol. 11, no. 81, **(2001)**.
[2] N. Fu and X. Y. Peng, "K-Hough underdetermined blind mixing model recovery algorithm", Journal of Electronic Measurement and Instrument, vol. 5, no. 22, **(2008)**.
[3] B. H. Tan and S. L. Xie, "Underdetermined blind separation based on source signals' number estimation", Journal of Electronics & Information Technology, vol. 4, no. 30, **(2008)**.
[4] G. X. Zhou, Z. Y. Yang, S. L. Xie and J. M. Yang, "Mixing matrix estimation from sparse mixtures with unknown number of sources", IEEE Transactions on Neural Networks, vol. 2, no. 22, **(2011)**.
[5] D. Z. Peng and Y. Xiang, "Underdetermined blind sources separation based on relaxed sparsity condition of sources", IEEE Transactions on Signal Processing, vol. 2, no. 57, **(2009)**.
[6] S. G. Kim and C. D. Yoo, "Underdetermined blind source separation based on subspace representation", IEEE Transactions on Signal Processing, vol. 7, no. 57, **(2009)**.
[7] Y. Q. Li, S. Amari, A. Cichochi, D. W. C. Ho and S. L. Xie, "Underdetermined blind source separation based on sparse representation", IEEE Transactions on Signal Processing, vol. 2, no. 54, **(2006)**.
[8] P. Bofill, "Identifying single source data for mixing matrix estimation in instantaneous blind source separation", Artificial Neural Networks. Springer Berlin Heidelberg, **(2008)**, pp. 759-767.
[9] V. G. Reju, S. N. Koh and I. Y. Soon, "An algorithm for mixing matrix estimation in instantaneous blind source separation", Signal Processing, vol. 9, no. 89, **(2009)**.
[10] T. B. Dong, Y. K. Lei and J. S. Yang, "An algorithm for underdetermined mixing matrix estimation", Neurocomputing, vol. 15, no. 104, **(2013)**.
[11] S. L. Xie, L. Yang, J. M. Yang, G. X. Zhou and Y. Xiang, "Time-frequency approach to underdetermined blind source separation", IEEE Transactions on Neural Networks and Learning Systems, vol. 2, no. 12, **(2012)**.
[12] Z. T. Cui and K. Jian, "A new elgorithm to estimate mixing-matrix of underdetermined blind signal separation", Proceedings of Eighth International Conference on Computational Intelligence and Security, **(2012)** November 17-18, Hainan, China.

Authors

Sun Jiedi, She received her M.S degree (2001) in Circuit and System from Yanshan University and her Ph.D. degree (2008) in Precision Instrument and Machinery from Tianjin University. Now she is an Associate Professor in School of Information Science and Engineering, Yanshan University. Her main research interests include Blind source separation and application, complex vibration signals processing and recognition and Pipeline leak detection and pre-warning system.

LI Yuxia, She received the B.S degree in Electronic Information Engineering (2012) from Yanshan University. She is now a postgraduate of School of Information Science and Engineering, Yanshan University. Her research areas focus on: vibration signal processing, blind source separation and application.

Wen Jiangtao, He received his M.S degree (2003) in Measurement from Yanshan University and his Ph.D. degree (2009) in Instrumentation Science and Technology from Tsinghua University. Now he is an Associate Professor in School of Electronical Engineering, Yanshan University. His main research interests include complex vibration signals processing and recognition and Pipeline leak detection and pre-warning system.

Yan Shengnan, She received her her Ph.D. degree (2010) in Communication and Information System, from Beijing University of Posts and Telecommunications. Now she is a lecture in School of Information Science and Engineering, Yanshan University. Her main research interests include Blind source separation and application.

